

UCSF

UC San Francisco Previously Published Works

Title

Ectopic uterine tissue as a chronic pain generator

Permalink

<https://escholarship.org/uc/item/650489h6>

Authors

Alvarez, P
Chen, X
Hendrich, J
[et al.](#)

Publication Date

2012-12-01

DOI

10.1016/j.neuroscience.2012.08.033

Peer reviewed

Published in final edited form as:

Neuroscience. 2012 December 6; 225: 269–282. doi:10.1016/j.neuroscience.2012.08.033.

Ectopic uterine tissue as a chronic pain generator

Pedro Alvarez^{1,3}, Xiaojie Chen^{1,3}, Jan Hendrich^{1,3}, Juan C. Irwin^{4,5}, Paul G. Green^{1,3}, Linda C. Giudice^{4,5}, and Jon D. Levine^{1,2,3}

¹Department of Oral and Maxillofacial Surgery; University of California San Francisco, San Francisco, California, USA.

²Department of Medicine; University of California San Francisco, San Francisco, California, USA.

³Division of Neuroscience; University of California San Francisco, San Francisco, California, USA.

⁴Department of Obstetrics, Gynecology and Reproductive Sciences; University of California San Francisco, San Francisco, California, USA.

⁵Center for Reproductive Sciences; University of California San Francisco, San Francisco, California, USA.

Abstract

While chronic pain is a main symptom in endometriosis, the underlying mechanisms and effective therapy remain elusive. We developed an animal model enabling exploration of ectopic endometrium as a source of endometriosis pain. Rats were surgically implanted with autologous uterus in the gastrocnemius muscle. Within two weeks, visual inspection revealed the presence of a reddish-brown fluid filled cystic structure at the implant site. Histology demonstrated cystic glandular structures with stromal invasion of the muscle. Immunohistochemical studies of these lesions revealed the presence of markers for nociceptor nerve fibers and neuronal sprouting. Fourteen days after surgery rats exhibited persistent mechanical hyperalgesia at the site of the ectopic endometrial lesion. Intralesional, but not contralateral, injection of progesterone was dose-dependently antihyperalgesic. Systemic administration of leuprolide also produced antihyperalgesia. *In vivo* electrophysiological recordings from sensory neurons innervating the lesion revealed a significant increase in their response to sustained mechanical stimulation. These results are consistent with clinical and pathologic findings observed in patients with endometriosis, compatible with the ectopic endometrium as a source of pain. This model of endometriosis allows mechanistic exploration at the lesion site facilitating our understanding of endometriosis pain.

Keywords

endometriosis; chronic pain; progesterone; leuprolide; nociceptors; mechanical hyperalgesia

© 2012 IBRO. Published by Elsevier Ltd. All rights reserved.

Correspondence should be addressed to J.D.L. (jon.levine@ucsf.edu).

Publisher's Disclaimer: This is a PDF file of an unedited manuscript that has been accepted for publication. As a service to our customers we are providing this early version of the manuscript. The manuscript will undergo copyediting, typesetting, and review of the resulting proof before it is published in its final citable form. Please note that during the production process errors may be discovered which could affect the content, and all legal disclaimers that apply to the journal pertain.

Competing financial interests

The authors declare that no conflict of interest exists in connection with this study.

1. Introduction

Endometriosis, a chronic pain syndrome associated with the presence of ectopic endometrial glands and stroma, affects approximately 10% of women in their reproductive years (Giudice, 2010). Most characteristically, pain associated with endometriosis is exacerbated by mechanical stimuli, associated with physical activity, generating symptoms of dyspareunia (painful sexual intercourse), dyschezia (painful defecation), dysuria (painful urination) and low back pain (Giudice, 2010; Roman et al., 2011). This pain can occur unpredictably, be related to the menstrual cycle or can be continuous (Giudice, 2010).

Pain is more common or severe if lesions have a cystic appearance, are located at certain anatomical sites and when tissue penetration is deep (Fauconnier et al., 2002; Dai et al., 2012). And, some clinical studies indicate a positive association between pain symptoms and lesions observed at surgical exploration (Porpora et al., 1999). Unfortunately, available medical and surgical treatments for endometriosis pain provide only limited relief, with pain recurring in up to 50% of women within 6 to 12 months after completion of treatment (Giudice, 2010).

To explore the pathophysiology of endometriosis and to assay potential therapies, preclinical models have been developed. Most of these models are based on surgically implanted uterus ectopically, in the peritoneal cavity (Vernon and Wilson, 1985). Using this model in the rat, nociceptive responses compatible with pain symptoms observed in human endometriosis have been reported (Berkley et al., 2005), leading to the suggestion of the involvement of neuronal (Berkley et al., 2005) and immune (Umezawa et al., 2008) elements, as observed in human endometriosis (Giudice, 2010). However, while the relief of pain provided by surgical excision of symptomatic lesions (Giudice, 2010; Jacobson et al., 2009) and activity-induced pain symptoms (Giudice, 2010; Roman et al., 2011) strongly suggest a prominent role for peripheral mechanisms in endometriosis pain, there are no studies directly exploring the role of peripheral sensory processing in endometriosis pain. This results, in part, from the absence of preclinical models allowing direct stimulation of lesions and local interventions to modulate nociceptive processing or the ability to record neuronal activity arising from ectopic endometrial lesions. We report a new preclinical model of endometriosis pain in which one can explore underlying mechanisms and the evaluation of mechanism-based therapies to determine if they act at the site of an endometriosis lesion.

2. Experimental procedures

2.1. Animals

Adult female Sprague Dawley rats (200–220 g; Charles River, Hollister, CA, USA) were used in these experiments. They were housed in the Animal Care Facility at the University of California San Francisco, under environmentally controlled conditions (lights on 07:00–19:00 h; room temperature 21–23°C) with food and water available *ad libitum*. Upon completion of experiments, rats were killed by pentobarbital overdose followed by cervical dislocation. Animal care and use conformed to NIH guidelines (NIH Guide for the Care and Use of Laboratory Animals). The University of California San Francisco Committee on Animal Research approved all experimental protocols. Concerted effort was made to minimize number and suffering of experimental animals.

2.2. Chemicals

Unless otherwise stated, all chemicals used in these experiments were obtained from Sigma-Aldrich (St. Louis, MO, USA).

2.3. Determination of estrous cycle phases

The phase of the estrous cycle was assessed daily (8:00 to 9:00 AM). Briefly, rats were gently restrained and 20 μ l of NaCl 0.9% flushed 3–4 times into the vaginal cavity. The resulting fluid was then placed onto a slide and observed unstained at 100 \times magnification. The diagnostic criteria used to determine the cycle phase has been previously reported (Marcondes et al., 2002): in proestrus a predominance of round nucleated (epithelial) cells is observed; in estrus a predominance of polygonal/irregular anucleated (cornified) cells is observed; in diestrus a predominance of small round (neutrophil) cells is observed and in metestrus a similar proportion of small round cells, cornified cells and epithelial cells is observed.

2.4. Surgical induction of muscle endometriosis

In general terms, our model of surgically-induced muscle endometriosis was adapted from that used to induce peritoneal endometriosis in the rat (Vernon and Wilson, 1985). Only rats in proestrus were used for endometrial implantation surgery. Rats were anesthetized with a mixture of ketamine hydrochloride and xylazine (80 and 6 mg/kg, s.c., respectively) and anesthesia was maintained with isoflurane (1.5% in 98.5% oxygen). The fur on the abdominal and left calf regions were clipped and disinfected, and a midline abdominal anesthetic block performed by injecting 0.25% bupivacaine (0.2 ml, s.c.). Under aseptic conditions a midline incision approximately 4 cm in length was performed. After laparotomy, the abdominal cavity was examined and the right uterine horn identified, exposed and isolated using a sterilized cotton roll. With the aid of a surgical microscope, the right uterine artery and vein, and the uterine vessels from the ovarian artery were ligated at the level of the transition of the uterine horn to the oviduct, with a 5-0-nylon suture. This procedure was repeated 1 cm distally. The uterine horn bounded by these ligatures was sectioned perpendicularly to its axis, and a 1 cm segment removed and immediately placed in a Petri dish containing 0.9% NaCl. The distal stump of the uterine horn was then tied with 5-0 nylon suture. After confirming hemostasis, the musculature of the abdominal wall was closed with single crossed stitches and the skin incision closed with horizontal mattress stitches, using 5-0 nylon. The excised uterine tissue was measured with a millimeter scale and opened longitudinally; a full thickness 3 \times 3 mm square of uterine tissue was then removed and kept in physiologic saline. To perform the implant, the *biceps femoris* muscle was exposed by means of a 2 cm skin incision perpendicular to the long axis of the calf. Then, a 1 cm incision was performed in the *b. femoris* allowing exposure of the underlying gastrocnemius muscle. With the aid of a surgical microscope, the square of uterine tissue was sutured to the surface of the gastrocnemius muscle applying three to four single stitches using 5-0 nylon with the endometrial portion of the uterine tissue contacting the gastrocnemius muscle. After checking for hemostasis, the *b. femoris* muscle was closed with single stitches and the skin with single crossed stitches, using 5-0 nylon. The sham surgical procedure was similar but the implant sutured to the surface of the gastrocnemius muscle consisted of a 3 \times 3 mm square of peritoneal fat instead of uterine tissue. Postoperative recovery was assessed daily. Return of normal estrus cyclicity was found within 1 week of the procedure.

2.5. Measurement of muscle hyperalgesia

Mechanical nociceptive threshold in the gastrocnemius muscle was quantified using a digital force transducer (Chatillon DFI2; Amtek Inc., Largo, FL, USA) with a custom-made 7 mm diameter probe (Alvarez et al., 2010). Rats were lightly restrained in a cylindrical acrylic holder with lateral slats that allows for easy access to the hind limb and application of the force transducer probe to the site of implantation in the belly of the gastrocnemius muscle. The nociceptive threshold was defined as the force, in milliNewtons, required to produce a

flexion reflex in the hind leg. Baseline withdrawal threshold was defined as the mean of 3 readings taken at 5-min intervals.

2.6. Intralesional and systemic injections

Rats were briefly anesthetized with 2.5 % isoflurane to facilitate the injection of progesterone (Calbiochem[®], La Jolla, CA, USA) into the endometrial implant located in the gastrocnemius muscle (20 μ l). The injection site was previously shaved and scrubbed with alcohol. The precise location of the uterine implant was identified by palpation and the tip of the needle directed to the base of the implant. Immediately after injections the skin puncture site was marked with a fine-tip indelible ink pen, so that the mechanical nociceptive threshold of the underlying injection site in the muscle could be repeatedly tested. Solutions of progesterone (1 and 3 μ g/ μ l dissolved in 10% ethanol in NaCl 0.9%) were freshly prepared immediately before injection. For systemic injections, rats were briefly anesthetized with 2.5 % isoflurane and 0.25 ml of freshly prepared leuprolide acetate solution (concentration 4 mg/ml in sterile-filtered PBS containing 0.5% bovine serum albumin) were injected subcutaneously (s.c.) in the base of the neck.

2.7. Single fiber *in vivo* electrophysiology

Rats were anesthetized with sodium pentobarbital (initially 50 mg/kg, intraperitoneally, with additional doses given to maintain areflexia throughout the experiment), their trachea cannulated to maintain patency of their upper airway and heart rate monitored. Anesthetized animals were positioned on their right side and an incision made on the dorsal skin of the left leg, between the mid-thigh and calf. Then the *b. femoris* muscle was partially removed to expose the sciatic nerve and gastrocnemius muscle. The edges of the incised skin were fixed to a metal loop to provide a pool that was filled with warm mineral oil that bathed the sciatic nerve and gastrocnemius muscle.

The sciatic nerve was cut proximally to prevent flexor reflexes during electrical stimulation of sensory neurons. Fine fascicles of axons were then dissected from the distal stump, and placed on a recording electrode. Single units, first detected by mechanical stimulation of the gastrocnemius muscle with a small blunt-tipped glass bar, were subsequently confirmed by electrical stimulation of the mechanical receptive field, according to the waveform of its action potentials. Bipolar stimulating electrodes were then placed and held on the center of the receptive field of the muscle afferent by a micromanipulator (Narishige model MM-3, Tokyo, Japan). Conduction velocity of each fiber was calculated by dividing the distance between the stimulating and recording electrodes by the latency of the electrically evoked action potential. All recorded muscle afferents had conduction velocities in the range of type III (conduction velocity 2.5–30 m/s) or type IV (conduction velocity <2.5 m/s) fibers (Diehl et al., 1993). Mechanical threshold, determined with calibrated von Frey hairs (VFH Ainsworth, London, UK), was defined as the lowest force that elicited at least 2 spikes within 1 second, in at least 50% of trials. Sustained (60 s) suprathreshold (10 g) mechanical stimulation was accomplished by use of a mechanical stimulator that consisted of a force-measuring transducer (Entran, Fairfield, NJ, USA) with a blunt plastic tip that was applied by a micromanipulator (BC-3 and BE-8, Narishige) on the center of the afferent's receptive field for 60 seconds. Neural activity and timing of stimulus onset and termination were monitored and stored on a computer with a Micro 1401 interface (CED, Cambridge, UK) and analyzed off-line with Spike2 software (CED).

2.8. Labeling of DRG neurons innervating the endometrial cyst

The dorsal root ganglion (DRG) neurons innervating the endometrial cyst (uterine tissue-implanted rats) and gastrocnemius muscle (control rats) were identified by their uptake of the retrograde tracer 1,1'-dioctadecyl-3,3',3'-tertamethylindocarbocyanine perchlorate

(DiI). Three weeks after ectopic uterine tissue implantation, rats were anesthetized (isoflurane, 3%), and incision of the skin and *b. femoris* muscle made to expose the gastrocnemius muscle and the cystic lesion. A 30-g needle was inserted into the gastrocnemius muscle or the cystic cavity of the lesion and 1 μ l DMSO containing 2% DiI was slowly injected. The injection was performed over 2 min, followed by observation for 1 min to ensure that dye was not leaking from the site of injection. The skin was then sutured and rats allowed to recover.

2.9. DRG cell-culture

DRGs were surgically removed from rats 5–8 days after DiI injection. Under isoflurane anesthesia, rats were decapitated and the vertebral column excised. The column was then opened up on the ventral side, and L4-L5 DRGs were removed and de-sheathed. Ganglia were treated with collagenase (0.125% in Neurobasal-A medium, Invitrogen, Carlsbad, CA) for 90 min at 37°C, and then treated with trypsin (0.25% in Ca²⁺- and Mg²⁺-free PBS, Invitrogen) for 10 min, followed by trituration (in Neurobasal-A) to produce a single-cell suspension. The suspension was centrifuged at 1000 RPM and re-suspended in Neurobasal-A medium supplemented with 50 ng/ml nerve growth factor, 100 U/ml penicillin/streptomycin and B-27 (Invitrogen). Cells were then plated on coverslips coated with poly-DL-ornithine (0.1 mg/ml) and laminin (5 μ g/ml; Invitrogen), and incubated at 37°C in 5% CO₂.

2.10. *In vitro* electrophysiology

Electrophysiology was performed using an Axopatch 200A amplifier and a pCLamp 8.2 software (Molecular Devices, Sunnyvale, CA, USA). DRG neurons were subjected to voltageclamp after 2–36 hr in culture. Coverslips were incubated with FITC-conjugated *Griffonia simplicifolia* isolectin B4 for 10 min before recording. Cells were held in the whole-cell configuration at –60 mV following seal formation (seal resistance > 1G Ω). Whole-cell capacitance and series resistance were compensated (80%) using the amplifier circuitry. Cells with a series resistance >10 M Ω were not used for experimentation.

The external solution, configured to minimize Na⁺ and Ca²⁺ currents, contained (in mM): choline chloride (130); KCl (5); CaCl₂ (2.5); MgCl₂ (0.6); HEPES (5); glucose (10); CdCl₂ (1). The solution was altered to pH 7.4 with TrisBase and 320 mOsm with sucrose. The pipette solution contained (in mM): KCl (30); K-MES (110); MgCl₂ (1); HEPES (10); EGTA (0.1), altered to pH 7.2 and 310 mOsm.

Traces representing predominantly delayed rectifier (I_{DR}) and A-type (I_A) potassium currents were obtained by the sequential bath perfusion of external solution containing 25 mM TEA and 5 mM 3,4-diaminopyridine, respectively. Current-voltage (I-V) traces were normalized to cell capacitance, as determined from the amplifier circuitry. Data were analyzed and plotted using Origin 6.1 software (OriginLab, Northampton, MA, USA).

2.11. Tissue harvesting, immunostaining and histology

At appropriate postsurgical times (indicated in the Results section), rats were deeply anesthetized (urethane, 1.5 g/kg, ip) and transcardially perfused with warm (30°C) heparinized saline (25 IU heparin/ml) followed by cold (10°C) phosphate-buffered solution (PBS, 0.1 M, pH 7.6) containing 4% paraformaldehyde and 0.03% picric acid for 15 min. The implanted gastrocnemius muscle and adherent endometrial cyst were removed and then cryoprotected in 30% sucrose PBS at 4°C and left overnight. Fifty μ m thick sections of implanted muscle were cut on a freezing microtome (Leica Model CM 3050S, Nussloch, Germany) and thaw mounted on glass slides.

Mounted tissue sections were washed 3 times in PBS and incubated in 2% normal goat serum (NGS) in PBS - 0.3% Triton X 100 (NGS-PBS-TX) for 30 min at room temperature and then incubated with a mouse anti-growth associated protein 43 (GAP 43) antibody (1:1000, Abcam, Cambridge, MA, USA) in NGS-PBS-TX for 48 hrs at 4°C. To detect nociceptor markers, sections were incubated with either a rabbit antibody anti calcitonin gene-related peptide (CGRP, 1:2000, Sigma-Aldrich, St. Louis, MO, USA) 48 hrs at 4°C, or with the FITC-conjugated *Griffonia simplicifolia* isolectin B4 (FITC-IB4, diluted to 1 µg/µl in PBS and used 1:500, Invitrogen) for 2 hrs at room temperature, in NGS-PBS-TX. To reveal GAP-43 immunoreactivity, sections were incubated in a biotinylated goat anti-mouse IgG (1:500, Jackson ImmunoResearch, West Grove, PA, USA) and then in FITC-conjugated streptavidin (1:500, CALTAG Laboratories, Burlingame, CA, USA) in NGS-PBS-TX for 2 hrs at room temperature. To reveal CGRP immunoreactivity, sections were incubated in an Alexa 594-conjugated goat anti-rabbit antibody (1:500, Invitrogen) in NGS-PBS-TX for 2 hrs at room temperature. After 3 washes in PBS, staining was verified in wet sections using an epifluorescence microscope (Nikon Eclipse 80i, Tokyo, Japan). Sections were let dry and coverslipped with a DAPI (4',6-diamidino-2-phenylindole) containing anti-fade mounting media (Prolong[®] Gold, Invitrogen). Standard hematoxylin and eosin staining was used for the assessment of the histological features of lesions in implanted muscles. Briefly, 8 µm sections were stained with hematoxylin, rinsed in running tap water and stained with eosin. Sections were then dehydrated in graded alcohols, cleared in xylene and coverslipped with a histological mounting media.

For immunohistochemical analysis of vimentin and cytokeratin expression in endometrial implants, 8 µm cryostat sections were immunostained using mouse monoclonal antibodies to vimentin (clone V9, Sigma-Aldrich) or cytokeratin 18 (ab 668, Abcam, Cambridge, MA, USA). Cytokeratin immunostaining was preceded by antigen retrieval incubating sections in a pH 6.0 citrate-based antigen unmasking solution (Vector Laboratories, Burlingame, CA, USA) at 95°C for 15 min, followed by washing twice with distilled water and once with PBS. Sections were first incubated with 2.5% normal goat serum in PBS for 1h, then with the primary antibody diluted 1:100 in PBS + 2.5% normal goat serum for 1 hr, followed by three washes in PBS + 0.1% Tween 20, and finally with Alexa Fluor 488-conjugated goat anti-mouse IgG (Invitrogen) diluted 1:250 for 1 hr. After final washing as above, wet sections were coverslipped with a DAPI-containing anti-fade mounting medium (Vectashield[®], Vector Laboratories), viewed on a Zeiss Axio Observer D1 epifluorescence microscope (Carl Zeiss, Thornwood, NY, USA) and images captured with an AxioCam MRm using AxioVision software.

2.12. Statistical analysis

Group data are expressed as mean ± SEM of *n* independent observations. Statistical comparisons were made using GraphPad Prism 5.0 statistical software (GraphPad Software, Inc., La Jolla, CA, USA). The Student's t-test was used to compare 1 or 2 independent samples, whereas analysis of variance (ANOVA) followed by Tukey's or Dunnett's multiple comparison tests were used for comparing multiple treatments. Data were tested for normality using the D'Agostino and Pearson omnibus normality test; if data did not pass the normality test for Gaussian distribution, Welch correction for the Student's t-test was used. Mann-Whitney's test was used for comparison of mechanical threshold data obtained from single fiber *in vivo* electrophysiology. *P* < 0.05 was considered statistically significant.

3. Results

3.1. Induction of endometriosis

Rats recovered uneventfully from surgical intervention, with those submitted to autologous uterine tissue implant only distinguishable by the presence of a small mass-like lesion in the left calf region. Surgical inspection of such lesion revealed the presence of a cystic structure in the gastrocnemius muscle at the implant site, in all animals. Surgical exposure of the cyst revealed a reddish-brown fluid filling the cyst's cavity (Fig. 1A). A profusion of fine blood vessels issuing from surrounding epimysium was evident in the surface of the cyst. Histologic analysis of hematoxylin-eosin stained samples confirmed the presence of cystic glandular structures and stromal invasion of the underlying muscle (Fig. 1B, C).

3.2. Mechanical hyperalgesia

Twelve days after surgical implantation with either autologous uterus (endometriosis model) or peritoneal fat pad (sham control), on the left gastrocnemius muscle, rats exhibited significant decrease in pain threshold to mechanical stimulation (mechanical hyperalgesia) at the site of the implant ($-54.2 \pm 2.7\%$, $n = 11$, and $-36.2 \pm 7.2\%$, $n = 4$, respectively; one way ANOVA followed by Dunnett post-hoc test, $P < 0.001$, Fig. 1D). However, at postoperative day fourteen rats submitted to the endometriosis model ($-48.8 \pm 3.3\%$, $n = 12$), but not control rats ($-2.2 \pm 2.5\%$, $n = 4$), exhibited a marked mechanical hyperalgesia in the operated hind limb compared to pre-surgical baseline (one way ANOVA followed by Dunnett post-hoc test, $P < 0.001$, Fig. 1D). This hyperalgesia remained unattenuated on postoperative day 27 ($-44.4 \pm 1.8\%$, $n = 8$, one way ANOVA followed by Dunnett post-hoc test, $P < 0.001$, Fig. 1D). To evaluate whether the persistent hyperalgesia observed in our model of endometriosis pain fluctuated with the stage of the rat's reproductive cycle, mechanical threshold values were matched to every stage of the estrus cycle as diagnosed by daily vaginal cytology. No significant differences in the amplitude of mechanical hyperalgesia were observed over the estrus cycle ($P > 0.05$, Fig. 1E).

3.3. Intralesional progesterone inhibits hyperalgesia associated with uterine implants

Given that most effective medical treatments for endometriosis pain are based on progesterone or progestin administration (McCormack, 2010), we assessed whether the hyperalgesia observed in our model of endometriosis pain is sensitive to locally administered progesterone. Three weeks after surgically implanting uterine tissue, rats received a single intralesional injection of progesterone (1 or 3 $\mu\text{g}/20\ \mu\text{l}$) and the mechanical nociceptive threshold of the implanted area was evaluated (Fig. 1F, G). The intralesional injection of progesterone dose-dependently inhibited the mechanical hyperalgesia. The maximal antinociceptive effect was observed 4 hours after the injection of either 1 μg (-47 ± 2.2 versus -36.9 ± 2.4 [$n = 8$], repeated measures ANOVA followed by Dunnett post-hoc test, $P < 0.001$, Fig. 1F), or 3 μg of progesterone (-50.5 ± 2.5 versus -18.2 ± 3.2 [$n = 9$], repeated measures ANOVA followed by Dunnett post-hoc test, $P < 0.001$, Fig. 1G). In contrast, contralateral injection of progesterone (1 or 3 $\mu\text{g}/20\ \mu\text{l}$) did not produce a significant effect on mechanical hyperalgesia (Fig. 1H, I).

3.4. Systemic leuprolide inhibits hyperalgesia associated with uterine implants

The gonadotropin-releasing hormone (GnRH) receptor agonists are currently used clinically for endometriosis pain (Giudice, 2010; Streuli et al., 2012). To evaluate whether our model is sensitive to this class of therapeutic agents, we administered the GnRH receptor agonist leuprolide acetate (1 mg) in our model of endometriosis pain. One day after s.c. injection of leuprolide an increase in mechanical hyperalgesia in the implanted area was observed (-62.6 ± 4.2 versus $-47.5 \pm 1.8\%$, [$n = 4$], repeated measures ANOVA followed by Dunnett

posthoc test, $P < 0.01$, Fig. 2). Thereafter, this mechanical hyperalgesia decreased progressively, and by day 5 after leuprolide injection there was a significant antihyperalgesia compared to preleuprolide thresholds (-29.3 ± 2.8 [$n = 4$], repeated measures ANOVA followed by Dunnett posthoc test, $P < 0.001$, Fig. 2). Such antinociceptive effect persisted at least until day 7 after leuprolide s.c. injection (-36.4 ± 2.7 [$n = 4$], repeated measures ANOVA followed by Dunnett post-hoc test, $P < 0.05$, Fig. 2).

3.5. Structural features and sensory innervation of the lesion

Immunofluorescence studies of endometriosis-like lesions revealed the presence of both stromal and glandular cellular elements, typical components of eutopic endometrium and a hallmark of endometriosis lesions (Eyster et al., 2002; Starzinski-Powitz et al., 1998). Immuno-labeling to vimentin in endometrial stromal fibroblasts and to cytokeratin 18 in endometrial surface epithelium was observed in eutopic uterus (Fig. 3A, B). Endometriosis-like cystic lesions also exhibited vimentin reactivity in endometrial stromal fibroblasts and endomysium (Fig. 3C), with lack of immuno-labeling in skeletal muscle fibers. These lesions also exhibited epithelial cells immunopositive to cytokeratin 18 surrounding the lumen of cystic structures (Fig. 3D). An extensive invasion of endometrial stromal fibroblasts to the endomysium, surrounding skeletal muscle fibers, was also observed (Fig. 3E–H).

Given that many studies have reported the presence of peptidergic nerve fibers immunopositive to calcitonin gene related peptide (CGRP) innervating endometriosis lesions in patients affected with chronic pelvic pain (Wang et al., 2009), we evaluated for the presence of CGRP-positive fibers in our endometriosis model. Indirect immunofluorescence revealed the presence of abundant CGRP-positive fibers surrounding and penetrating into the wall of the cyst (Fig. 4A–C). Since most tissues, including uterus (Papka et al., 2005), are also innervated by a subpopulation of nociceptors that binds isolectin B4 (IB4), we studied whether IB4-positive fiber-like structures were also present in the uterus implant-induced lesion. Staining of lesions with FITC-conjugated IB4 revealed fiber-like structures innervating the base of the ectopic endometrial cyst (Fig. 4D–F). Interestingly, CGRP-positive fiber-like structures also exhibited expression of the marker for neuronal sprouting, growth-associated protein 43 (GAP43) (Benowitz and Routtenberg) (Fig. 4G–I).

3.6. Sensitized nociceptors in endometriosis-like lesions

Two weeks after implantation surgery, the peripheral receptive field of sensory neurons innervating the uterine implant and adjacent gastrocnemius muscle was tested using von Frey monofilaments. The conduction velocity of muscle afferents recorded in naïve rats (1.96 ± 0.24 m/s, $n = 20$) was not significantly different from that recorded in endometriosis rats (2.25 ± 0.23 m/s, $n = 19$, Student's t-test, with Welch's correction, $P = 0.398$, Fig. 5A). The mechanical threshold of muscle afferents recorded in endometriosis rats was also not significantly different from that recorded in naïve controls (1.06 ± 0.13 mN, $n = 19$, and 1.24 ± 0.13 mN, $n = 20$, respectively; $P = 0.477$, Student's t-test with Welch's correction Fig. 5B). The excitability of muscle nociceptors from rats with endometriosis-like lesions and naïve controls was examined by evaluating their response to a sustained (60 s) suprathreshold (10 g) von Frey filament stimulus. In naïve (control) rats the response of muscle afferents to this sustained mechanical stimulation was 312.5 ± 92.6 action potentials/60 s stimulus ($n = 20$, Fig. 5C, D). In rats submitted to the endometriosis model, this response was significantly increased (749.1 ± 207 action potentials/60 s stimulus, $n = 19$, $P = 0.028$, Fig. 5C, D). The analysis of the time course of the response to sustained mechanical stimulation showed a non-significant increase in the number of spikes during the first 10 s after application of the stimulus (165.7 ± 31 action potentials/10 s stimulus in control rats [n

= 20] compared to 232.7 ± 138.7 action potentials/10 s stimulus in rats implanted with ectopic uterine tissue. [n = 19], $P = 0.111$, Student's t-test with Welch's correction, Fig. 5C–F). However, the number of spikes recorded during the last 50 s after application of the stimulus was significantly increased in rats implanted with uterine tissue (146.8 ± 74.1 action potentials/50 s stimulus in control rats [n = 20] compared to 516.4 ± 171.1 action potentials/50 s stimulus in rats implanted with ectopic uterine tissue [n = 19], $P = 0.025$ Student's t-test with Welch's correction, Fig. 5C–F).

3.7. *In vitro* electrophysiology of DRG neurons that innervated ectopic endometrium

DiI labeled neurons that innervated endometriosis lesions were identified in cultured DRG neurons under epifluorescence illumination, and classified as IB4-positive or IB-negative after staining with FITC-conjugated isolectin IB4 (Fig. 6A, B). Of note, the vast majority (>90%) of DiI-labeled DRG neurons observed in culture were IB4-positive. Since estrogen plays a central role in endometriosis pathophysiology (Giudice, 2010) and injected locally it produces mechanical hyperalgesia (Hucho et al., 2006), we determined whether electrophysiological differences in DRG neurons innervating ectopic endometrium observed *in vitro* are related to known effects of estrogen. Taking into account that the modulation of A-type potassium current has been implicated in persistent pain (Chien et al., 2007) and that $K_v4.3$ transcription and membrane trafficking in uterine tissue is reduced by estrogen (Song et al., 2001), we first focused *in vitro* electrophysiology studies on A-type potassium currents. Recordings of A-type (I_A) (Fig. 6C, D) and delayed rectifier currents (I_{DR}) (Fig. 6E, F) were obtained using specific blockers). The I_A (1.43 ± 0.44 nA) or I_{DR} (2.41 ± 0.52 nA) currents recorded from DRG neurons innervating ectopic endometrium showed no significant changes in the peak current with respect to those obtained from naïve (control) rats (I_A control 1.40 ± 0.56 nA, $P > 0.05$; I_{DR} control 2.86 ± 0.78 nA, $P > 0.05$; Fig. 6C–F).

4. Discussion

The heterogeneity of clinical presentations of endometriosis and the difficulty in monitoring progression of the disease, by non-invasive methods, make animal models an important tool for the study of underlying mechanisms of its pathogenesis, and pathophysiology of associated pain (Story, L. & Kennedy, 2004). Accordingly, several preclinical models of endometriosis have been developed, including those that involve the surgical implant of autologous uterine tissue in the peritoneal cavity of rodents (Vernon and Wilson, 1985; Berkley et al., 2005; Story and Kennedy, 2004). Such an approach produces cystic lesions and pain symptoms comparable to those observed in patients suffering from endometriosis (Berkley et al., 2005).

The presence of cystic endometriosis lesions in patients exhibiting pain and its relief (at least temporary) observed immediately after its surgical excision, points towards an important contribution of peripheral mechanisms in endometriosis pain (Jacobson et al., 2009). However, direct evidence about such a contribution is still lacking and most of the preclinical studies of endometriosis pain are based on the assessment of secondary hyperalgesia (Berkley et al., 2001; Cason et al., 2003; McAllister et al., 2009; McAllister et al., 2012) leading to gaps between functional and morphological findings. For instance, while nociceptor fibers are clearly present in cystic lesions 2 weeks after surgical implant of uterine tissue in the peritoneal cavity, vaginal hyperalgesia becomes significant only 2–3 weeks later (McAllister et al., 2012).

Since there are no animal models of endometriosis allowing the direct exploration of primary hyperalgesia, the electrophysiology of the innervation of the endometrial lesion and the effect of local modulatory interventions, we developed a model of endometriosis based on the implant of uterine tissue on the gastrocnemius muscle, a site that provides important

vascular support and potential for sensory innervation for the ectopic implant, and allows easy assessment of primary hyperalgesia. Of note, although skeletal muscle is far from the main tissue affected by endometriosis, several clinical reports have communicated cases of endometriosis affecting muscle, the cause of consultation being local muscle pain (Lipscomb et al., 2011; Giannella et al., 2010; Botha et al., 1991; Fambrini et al., 2010; Poli-Neto et al., 2009).

The presence of endometrial cells in the peritoneal cavity of endometriosis patients has been explained as a consequence of retrograde menstruation/transplantation from eutopic uterus (Sampson, 1927). Given the lack of menstruation in rodents, the pertinence of preclinical models of endometriosis developed in these species has been questioned (Story and Kennedy, 2004). However, while most women have retrograde menstruation, only a fraction is affected by endometriosis (Giudice, 2010). Furthermore, the theory of Sampson fails to explain the presence of subperitoneal endometriosis (deep endometriosis) and endometriosis in remote areas outside of the peritoneal cavity (Signorile and Baldi, 2010). Indeed, recent evidence indicates that abnormalities in female genital embryogenesis, mainly dislocation of primitive endometrial tissue outside of the uterine cavity, is a plausible cause of endometriosis (Signorile et al., 2012). Since the implant of endometrial cells by retrograde menstruation is not a necessary condition for the development of clinical endometriosis, the surgical implant of autologous endometrial tissue outside of, as well as within, the peritoneal cavity provides a valid approach for the study of endometriosis mechanisms.

Two weeks post-surgery, 100% of animals implanted in the gastrocnemius muscle with uterus tissue developed a cystic lesion, which contrasts with the lower rate of success reported for the induction of peritoneal endometriosis-like lesions (Cason et al., 2003; Nogueira Neto et al., 2007; Do Amaral et al., 2009). Particular characteristics of skeletal muscle as a tissue receptor might have contributed to the high rate of cystic lesion induction observed here. For instance, skeletal muscle is a well-known source of trophic factors (Meek et al., 2004; Sakuma and Yamaguchi, 2011) and the disposition of its basal lamina offers a microenvironment that, for tissue grafts, promotes cell adhesion to extracellular matrix (Sakuma and Yamaguchi, 2011).

The histological identity of cystic lesions was confirmed as ectopic endometrium by the presence of (stromal) vimentin- and (glandular) cytokeratin-like immunoreactivity. The presence of such markers, especially vimentin, unveiled a deep infiltration of skeletal muscle by stromal cells issued from the uterine implant, consistent with previous findings of its up-regulation in endometriosis lesions (Eyster et al., 2002). On the other hand, the cytokeratin-like immunoreactivity exhibited by epithelial cells surrounding the lumen of cystic lesions confirms the invasive capacity of this phenotype, observed in human endometriosis (Starzinski-Powitz et al., 1998).

In agreement with previous reports (Berkley et al., 2005; McAllister et al., 2009) we also observed nerve fiber-like structures innervating the cystic lesions, which were positive for the markers of the two main nociceptor subpopulations, namely CGRP and IB4 (Snider and McMahon, 1998). While most of the DRG cells observed in culture were IB4-positive neurons, it must be stressed that both peptidergic (CGRP-positive) and IB4-positive nerve fiber-like structures were present in cystic lesions in our model of endometriosis. On the other hand, the IB4 staining in cystic lesions has not been studied in other rodent models of endometriosis, including the studies by Berkley and colleagues (Berkley et al., 2005; McAllister et al., 2012), making it hard to estimate the relative contribution of IB4-positive neurons in those previous studies. Of note, the proportion of IB4-positive neurons innervating viscera varies widely depending on the visceral tissue considered, from 7% in stomach (Thorton et al., 2005) to 58% in descending colon (Qian et al., 2009) a common site

of endometriosis lesions. Interestingly, a significant proportion of DRG cells innervating the uterus also innervate the colon (Li et al., 2008), with the latter exhibiting a high proportion of retrograde-labeled IB4-positive DRG cells (Qian et al., 2009). Evidence indicates that a significant proportion of nociceptors can be labeled with both; for example, antibodies directed to peptidergic markers and IB4-conjugated stains in DRG cells obtained from rats (Price and Flores, 2007). Indeed, most of primary afferent neurons innervating pelvic organs such as bladder are both IB4 and CGRP-positive (Hwang et al., 2005). Finally given that, for the cell body, the IB4 staining peptidergic neurons are likely to be the weakly IB4-positive (Fang et al., 2006), it is possibly the staining of their peripheral terminals may be difficult to detect.

GAP43 is an established marker of neuronal development, sprouting and plasticity (Benowitz and Routtenberg, 1997). In sensory neurons GAP43 is expressed in high levels not only during development but after lesion of peripheral nerves, it is selectively expressed in small-diameter sensory neurons (Woolf et al., 1990). Interestingly, GAP43 is overexpressed in nerve terminals of organs affected by chronic painful diseases (Freemont et al., 1997; Di Sebastiano et al., 1997), including endometriosis (Wang et al., 2009). Consistent with these reports, we observed GAP43 in endometriosis lesions in the rat, indicative of persistent nerve ingrowth.

Rats submitted to our endometriosis model also exhibited a persistent, intense mechanical hyperalgesia. Assessment of the nociceptive threshold at the site of the ectopic lesion demonstrated increased sensitivity corresponding to a primary mechanical hyperalgesia related to the implant of uterine tissue. Such mechanical hyperalgesia fits well with clinical features of endometriosis pain, usually related to mechanical stimuli being associated with dyspareunia, dyschezia, dysuria and low back pain (Giudice, 2010; Roman et al., 2011). However, in contrast to previous reports, in models demonstrating changes in nociceptive responses over the estrous cycle in a rat model of endometriosis pain (Berkley et al., 2005), we did not observe a significant change in nociceptive threshold. While aggravation of endometriosis pain during menses is a well-known symptom, it must be stressed that it can also be continuous in intensity (Giudice, 2010). Given that aromatase expression and local synthesis of estrogen is observable in endometriosis lesions (Huhtinen et al., 2012), and that medical interventions (GnRH agonists) or physiological processes (e.g. pregnancy) that disrupt gonadal production of estrogen inhibit endometriosis pain (Giudice, 2010; Streuli et al., 2012), estrogen produced by both the gonads and endometriosis lesions may contribute to mechanical hyperalgesia. Thus, the lack of the effect of the estrous cycle on nociceptive threshold might be explained by a high local production of estrogen. Since we performed a direct assessment of endometriosis lesion-induced pain (i.e., primary hyperalgesia was measured), local production of estrogen may mask the effect of variations in gonadal estrogen production, leading to a constant hyperalgesia regardless the phase of estrous cycle. Indeed, changes in pain behavior across the estrous cycle reported in other models of endometriosis are assessed in tissues not directly affected by lesions (i.e., secondary hyperalgesia). In these models decreased nociceptive thresholds are observed across the estrous cycle, with exception of estrous, a stage where the additive estrogen production (gonadal + endometriosis lesion) is absent (Cason et al., 2003). Conversely, such models of endometriosis pain exhibit higher secondary hyperalgesia when the additive estrogen production is higher (i.e., proestrus) (Cason et al., 2003).

The pain-related behavior induced by uterine implants in muscle was found to be sensitive to local administration of progesterone, an agent used clinically for the treatment of endometriosis pain (McCormack et al., 2010). A fast onset, dose-dependent and persistent antinociception was observed, and only local injections were able to produce such effects. Of note similar local analgesic effects have been reported in patients affected by carpal

tunnel syndrome pain (Milani et al., 2010; Ginanneschi et al., 2012). While the study of the mechanisms of the antinociceptive effect of progesterone on this model is beyond of the scope of this paper, one could speculate about the involvement of genomic and non-genomic effects. Among the non-genomic mechanisms, it is interesting to note that progesterone directly inhibits ATP-evoked P2X3 receptor-dependent inward currents (Fan et al., 2011), which are well-established players in muscle pain (Shinoda et al., 2008; Dessem et al., 2010). Long-lasting effects of progesterone may be related to additional genomic mechanisms, such as those involved in progesterone-induced inhibition of cytokine-mediated inflammation (Davies et al., 2004), which are known to contribute to endometriosis pain (Giudice, 2010; Umezawa et al., 2008; McKinnon et al., 2012).

We also explored the effects of another drug used clinically for endometriosis pain, the GnRH agonist leuprolide, in our model of endometriosis pain. Unexpectedly, one day after leuprolide administration, an increase in mechanical hyperalgesia was observed. This finding may be related to the “flare effect” induced by GnRH agonists, which consists in an initial temporal stimulation of the hypophysis-gonadal axis with rise in estrogen levels (Miller, 2000). Remarkably, such flare effect is associated to an increase of pain in endometriosis patients (Miller, 2000). Thereafter, a progressive and sustained attenuation of the mechanical hyperalgesia was observed. This observation, along with those about the lack of estrous cycle effect in our model of endometriosis pain, underline the prominent role of estrogen production by endometriosis lesions which might explain why the blockage of gonadal production of estrogen does not produce a complete control of endometriosis pain (Giudice, 2010). Of note, GnRH receptors are also present in endometriosis lesions and leuprolide inhibits the proliferation and increase the apoptosis index of cultured endometrial cells from endometriosis lesions (Borroni et al., 2000; Meresman et al., 2003). Thus, the contribution of such a direct effect in the antinociceptive effects of leuprolide observed here cannot be ruled out.

The down-regulation of K_v ion channels in sensory neurons is a well-known contributing factor to their sensitization. In particular, the decrease in A-type potassium currents has been implicated in mechanical hypersensitivity (Chien et al., 2007). In addition $K_v4.3$ expression – a major conduit of A-type current in sensory neurons (Phuket and Covarrubias, 2009) – is reduced in uterine tissue by estrogen (Song et al., 2001), a major player in endometriosis pathophysiology (Giudice, 2010). However, in recordings made from endometriosis lesion-innervating DRG neurons, A-type (or delayed rectifier) potassium currents did not exhibit any difference compared to those obtained from control animals. Thus, additional studies will be required to elucidate the ion channels that mediate enhanced nociceptor function associated with endometriosis.

5. Conclusions

In summary, rats submitted to extraperitoneal endometriosis exhibit a persistent primary mechanical hyperalgesia and enhanced nociceptor firing. Findings at surgical inspection, immunohistochemical studies and sensitivity of mechanical hyperalgesia to progesterone and leuprolide in these animals, are consistent with clinical and pathologic findings observed in patients suffering from endometriosis pain. These characteristics represent an advantage with respect to models of endometriosis pain based on assessment of secondary hyperalgesia (Berkley et al., 2001; Cason et al., 2003; McAllister et al., 2009; McAllister et al., 2012) (Fig. 7). Indeed, since our model allows easy access to the lesion site and the possibility to explore it by direct stimulation and recording of nerve fibers, and local administration of putative modulators (Fig. 7), it can be used to provide insight into chronic pain induced by endometriosis.

Acknowledgments

Authors thank D. Mendoza for excellent technical assistance. This work was funded by a US National Institutes of Health grant.

References

- Alvarez P, Levine JD, Green PG. Eccentric exercise induces chronic alterations in musculoskeletal nociception in the rat. *Eur J Neurosci*. 2010; 32:819–825. [PubMed: 20726881]
- Benowitz LI, Routtenberg A. GAP-43: an intrinsic determinant of neuronal development and plasticity. *Trends Neurosci*. 1997; 20:84–91. [PubMed: 9023877]
- Berkley KJ, Cason A, Jacobs H, Bradshaw H, Wood E. Vaginal hyperalgesia in a rat model of endometriosis. *Neurosci Lett*. 2001; 306:185–188. [PubMed: 11406326]
- Berkley KJ, Rapkin AJ, Papka RE. The pains of endometriosis. *Science*. 2005; 308:1587–1589. [PubMed: 15947176]
- Botha AJ, Halliday AE, Flanagan JP. Endometriosis in gluteus muscle with surgical implantation. A case report. *Acta Orthop Scand*. 1991; 62:497–499. [PubMed: 1950501]
- Borroni R, Di Blasio AM, Gaffuri B, Santorsola R, Busacca M, Viganò P, Vignali M. Expression of GnRH receptor gene in human ectopic endometrial cells and inhibition of their proliferation by leuprolide acetate. *Mol Cell Endocrinol*. 2000; 159:37–43. [PubMed: 10687850]
- Cason AM, Samuelson CL, Berkley KJ. Estrous changes in vaginal nociception in a rat model of endometriosis. *Horm Behav*. 2003; 44:123–131. [PubMed: 13129484]
- Chien LY, Cheng JK, Chu D, Cheng CF, Tsaur ML. Reduced expression of A-type potassium channels in primary sensory neurons induces mechanical hypersensitivity. *J Neurosci*. 2007; 27:9855–9865. [PubMed: 17855600]
- Dai Y, Leng JH, Lang JH, Li XY, Zhang JJ. Anatomical distribution of pelvic deep infiltrating endometriosis and its relationship with pain symptoms. *Chin Med J (Engl)*. 2012; 125:209–213. [PubMed: 22340547]
- Davies S, Dai D, Wolf DM, Leslie KK. Immunomodulatory and transcriptional effects of progesterone through progesterone A and B receptors in Hec50co poorly differentiated endometrial cancer cells. *J Soc Gynecol Investig*. 2004; 11:494–499.
- Dessem D, Ambalavanar R, Evancho M, Moutanni A, Yallampalli C, Bai G. Eccentric muscle contraction and stretching evoke mechanical hyperalgesia and modulate CGRP and P2X(3) expression in a functionally relevant manner. *Pain*. 2010; 149:284–295. [PubMed: 20207080]
- Di Sebastiano P, Fink T, Weihe E, Friess H, Innocenti P, Beger HG, Büchler MW. Immune cell infiltration and growth-associated protein 43 expression correlate with pain in chronic pancreatitis. *Gastroenterology*. 1997; 112:1648–1655. [PubMed: 9136844]
- Diehl B, Hoheisel U, Mense S. The influence of mechanical stimuli and of acetylsalicylic acid on the discharges of slowly conducting afferent units from normal and inflamed muscle in the rat. *Exp Brain Res*. 1993; 92:431–440. [PubMed: 8454007]
- Do Amaral VF, Dal Lago EA, Kondo W, Souza LC, Francisco JC. Development of an experimental model of endometriosis in rats. *Rev Col Bras Cir*. 2009; 36:250–255. [PubMed: 20076906]
- Eyster KM, Boles AL, Brannian JD, Hansen KA. DNA microarray analysis of gene expression markers of endometriosis. *Fertil Steril*. 2002; 77:38–42. [PubMed: 11779588]
- Fambrini M, Andersson KL, Campanacci DA, Vanzi E, Bruni V, Buccoliero AM, Pieralli A, Livi L, Scarselli G. Large-muscle endometriosis involving the adductor tight compartment: case report. *J Minim Invasive Gynecol*. 2010; 17:258–261. [PubMed: 20226421]
- Fan J, Lu Y, Yu LH, Zhang Y, Ni X, Burnstock G, Ma B. Progesterone rapidly attenuates ATP-evoked transient currents in cultured rat dorsal root ganglion neurons. *Pharmacology*. 2011; 87:36–44. [PubMed: 21178388]
- Fang X, Djouhri L, McMullan S, Berry C, Waxman SG, Okuse K, Lawson SN. Intense isolectin-B4 binding in rat dorsal root ganglion neurons distinguishes C-fiber nociceptors with broad action potentials and high Nav1.9 expression. *J Neurosci*. 2006; 26:7281–7292. [PubMed: 16822986]

- Fauconnier A, Chapron C, Dubuisson JB, Vieira M, Dousset B, Bréart G. Relation between pain symptoms and the anatomic location of deep infiltrating endometriosis. *Fertil Steril*. 2002; 78:719–726. [PubMed: 12372446]
- Freemont AJ, Peacock TE, Goupille P, Hoyland JA, O'Brien J, Jayson MI. Nerve ingrowth into diseased intervertebral disc in chronic back pain. *Lancet*. 1997; 350:178–181. [PubMed: 9250186]
- Giannella L, La Marca A, Ternelli G, Menozzi G. Rectus abdominis muscle endometriosis: case report and review of the literature. *J Obstet Gynaecol Res*. 2010; 36:902–906.
- Ginanneschi F, Milani P, Filippou G, Mondelli M, Frediani B, Melcangi RC, Rossi A. Evidences for antinociceptive effect of 17-alpha-hydroxyprogesterone caproate in carpal tunnel syndrome. *J Mol Neurosci*. 2012; 47:59–66. [PubMed: 22113360]
- Giudice LC. Clinical practice. Endometriosis. *N Engl J Med*. 2010; 362:2389–2398. [PubMed: 20573927]
- Hucho TB, Dina OA, Kuhn J, Levine JD. Estrogen controls PKCepsilon-dependent mechanical hyperalgesia through direct action on nociceptive neurons. *Eur J Neurosci*. 2006; 24:527–534. [PubMed: 16836642]
- Huhtinen K, Ståhle M, Perheentupa A, Poutanen M. Estrogen biosynthesis and signaling in endometriosis. *Mol Cell Endocrinol*. 2012; 358:146–154. [PubMed: 21875644]
- Hwang SJ, Oh JM, Valtschanoff JG. The majority of bladder sensory afferents to the rat lumbosacral spinal cord are both IB4- and CGRP-positive. *Brain Res*. 2005; 1062:86–91. [PubMed: 16263099]
- Jacobson TZ, Duffy JM, Barlow D, Koninckx PR, Garry R. Laparoscopic surgery for pelvic pain associated with endometriosis. *Cochrane Database Syst Rev*. 2009; 4:CD001300. [PubMed: 19821276]
- Li J, Micevych P, McDonald J, Rapkin A, Chaban V. Inflammation in the uterus induces phosphorylated extracellular signal-regulated kinase and substance P immunoreactivity in dorsal root ganglia neurons innervating both uterus and colon in rats. *J Neurosci Res*. 2008; 86:2746–2752. [PubMed: 18478547]
- Lipscomb GH, Givens VM, Smith WE. Endometrioma occurring in abdominal wall incisions after cesarean section. *J Reprod Med*. 2011; 56:44–46. [PubMed: 21366126]
- Marcondes FK, Bianchi FJ, Tanno AP. Determination of the estrous cycle phases of rats: some helpful considerations. *Braz J Biol*. 2002; 62:609–614. [PubMed: 12659010]
- McAllister SL, Dmitrieva N, Berkley KJ. Sprouted innervation into uterine transplants contributes to the development of hyperalgesia in a rat model of endometriosis. *PLoS One*. 2012; 7:e31758. [PubMed: 22363725]
- McAllister SL, McGinty KA, Resuehr D, Berkley KJ. Endometriosis-induced vaginal hyperalgesia in the rat: role of the ectopic growths and their innervation. *Pain*. 2009; 147:255–264. [PubMed: 19819623]
- McCormack PL. Dienogest: a review of its use in the treatment of endometriosis. *Drugs*. 2010; 70:2073–2088. [PubMed: 20964453]
- McKinnon B, Bersinger NA, Wotzkow C, Mueller MD. Endometriosis-associated nerve fibers, peritoneal fluid cytokine concentrations, and pain in endometriotic lesions from different locations. *Fertil Steril*. 2012; 97:373–380. [PubMed: 22154765]
- Meek MF, Varejão AS, Geuna S. Use of skeletal muscle tissue in peripheral nerve repair: review of the literature. *Tissue Eng*. 2004; 10:1027–1036. [PubMed: 15363160]
- Meresman GF, Bilotas M, Buquet RA, Barañao RI, Sueldo C, Tesone M. Gonadotropin-releasing hormone agonist induces apoptosis and reduces cell proliferation in eutopic endometrial cultures from women with endometriosis. *Fertil Steril*. 2003; 80(Suppl 2):702–707. [PubMed: 14505742]
- Milani P, Mondelli M, Ginanneschi F, Mazzocchio R, Rossi A. Progesterone - new therapy in mild carpal tunnel syndrome? Study design of a randomized clinical trial for local therapy. *J Brachial Plex Peripher Nerve Inj*. 2010; 5:11. [PubMed: 20420674]
- Miller JD. Quantification of endometriosis-associated pain and quality of life during the stimulatory phase of gonadotropin-releasing hormone agonist therapy: a double-blind, randomized, placebo-controlled trial. *Am J Obstet Gynecol*. 2000; 182:1483–1488. [PubMed: 10871469]

- Nogueira Neto J, Torres OJ, Coelho TM, Nunes JN Jr, Aguiar GC, Costa LK. Evaluation of the macroscopic growth degree of experimental endometriosis in rats. *Acta Cir Bras.* 2007; 22:8–11. [PubMed: 17505648]
- Papka RE, Hafemeister J, Storey-Workley M. P2X receptors in the rat uterine cervix, lumbosacral dorsal root ganglia, and spinal cord during pregnancy. *Cell Tissue Res.* 2005; 321:35–44. [PubMed: 15902498]
- Phuket TR, Covarrubias M. Kv4 channels underlie the subthreshold-operating A-type K-current in nociceptive dorsal root ganglion neurons. *Front Mol Neurosci.* 2009; 2:3. [PubMed: 19668710]
- Poli-Neto OB, Rosa-E-Silva JC, Barbosa HF, Candido-Dos-Reis FJ, Nogueira AA. Endometriosis of the soleus and gastrocnemius muscles. *Fertil Steril.* 2009; 91:1294.e13–1294.e15. [PubMed: 19152878]
- Porpora MG, Koninckx PR, Piazzè J, Natili M, Colagrande S, Cosmi EV. Correlation between endometriosis and pelvic pain. *J Am Assoc Gynecol Laparosc.* 1999; 6:429–434. [PubMed: 10548700]
- Price TJ, Flores CM. Critical evaluation of the colocalization between calcitonin gene-related peptide, substance P, transient receptor potential vanilloid subfamily type 1 immunoreactivities, and isolectin B4 binding in primary afferent neurons of the rat and mouse. *J Pain.* 2007; 8:263–272. [PubMed: 17113352]
- Qian AH, Liu XQ, Yao WY, Wang HY, Sun J, Zhou L, Yuan YZ. Voltage-gated potassium channels in IB4-positive colonic sensory neurons mediate visceral hypersensitivity in the rat. *Am J Gastroenterol.* 2009; 104:2014–2027. [PubMed: 19491827]
- Roman H, Vassiliev M, Gourcerol G, Savoye G, Leroi AM, Marpeau L, Michot F, Tuech JJ. Surgical management of deep infiltrating endometriosis of the rectum: pleading for a symptom-guided approach. *Hum Reprod.* 2011; 26:274–281. [PubMed: 21131296]
- Sakuma K, Yamaguchi A. The recent understanding of the neurotrophin's role in skeletal muscle adaptation. *J Biomed Biotechnol.* 2011; 2011:201696. [PubMed: 21960735]
- Sampson JA. Peritoneal endometriosis due to menstrual dissemination of endometrial tissue into the peritoneal cavity. *Am J Obstet Gynecol.* 1927; 14:422–469.
- Shinoda M, Ozaki N, Sugiura Y. Involvement of ATP and its receptors on nociception in rat model of masseter muscle pain. *Pain.* 2008; 134:148–157. [PubMed: 17521813]
- Signorile PG, Baldi A. Endometriosis: new concepts in the pathogenesis. *Int J Biochem Cell Biol.* 2010; 42:778–780. [PubMed: 20230903]
- Signorile PG, Baldi F, Bussani R, Viceconte R, Bulzomi P, D'Armiento M, D'Avino A, Baldi A. Embryologic origin of endometriosis: analysis of 101 human female fetuses. *J Cell Physiol.* 2012; 227:1653–1656. [PubMed: 21678420]
- Snider WD, McMahon SB. Tackling pain at the source: new ideas about nociceptors. *Neuron.* 1998; 20:629–632. [PubMed: 9581756]
- Song M, Helguera G, Eghbali M, Zhu N, Zarei MM, Olcese R, Toro L, Stefani E. Remodeling of Kv4.3 potassium channel gene expression under the control of sex hormones. *J Biol Chem.* 2001; 276:31883–31890. [PubMed: 11427525]
- Starzinski-Powitz A, Gaetje R, Zeitvogel A, Kotzian S, Handrow-Metzmacher H, Herrmann G, Fanning E, Baumann R. Tracing cellular and molecular mechanisms involved in endometriosis. *Hum Reprod Update.* 1998; 4:724–729. [PubMed: 10027626]
- Story L, Kennedy S. Animal studies in endometriosis: a review. *ILAR J.* 2004; 45:132–138. [PubMed: 15111732]
- Streuli I, de Ziegler D, Borghese B, Santulli P, Batteux F, Chapron C. New treatment strategies and emerging drugs in endometriosis. *Expert Opin Emerg Drugs.* 2012 in press.
- Thornton PD, Gerke MB, Plenderleith MB. Histochemical localisation of a galactose-containing glycoconjugate expressed by sensory neurones innervating different peripheral tissues in the rat. *J Peripher Nerv Syst.* 2005; 10:47–57. [PubMed: 15703018]
- Umezawa M, Sakata C, Tanaka N, Kudo S, Tabata M, Takeda K, Ihara T, Sugamata M. Cytokine and chemokine expression in a rat endometriosis is similar to that in human endometriosis. *Cytokine.* 2008; 43:105–109. [PubMed: 18595729]

- Vernon MW, Wilson EA. Studies on the surgical induction of endometriosis in the rat. *Fertil Steril.* 1985; 44:684–694. [PubMed: 4054348]
- Wang G, Tokushige N, Markham R, Fraser IS. Rich innervation of deep infiltrating endometriosis. *Hum Reprod.* 2009; 24:827–834. [PubMed: 19151028]
- Wang G, Tokushige N, Russell P, Dubinovsky S, Markham R, Fraser IS. Hyperinnervation in intestinal deep infiltrating endometriosis. *J Minim Invasive Gynecol.* 2009; 16:713–719. [PubMed: 19896597]
- Woolf CJ, Reynolds ML, Molander C, O'Brien C, Lindsay RM, Benowitz LI. The growth-associated protein GAP-43 appears in dorsal root ganglion cells and in the dorsal horn of the rat spinal cord following peripheral nerve injury. *Neuroscience.* 1990; 34:465–478. [PubMed: 2139720]

Highlights

Uterine tissue implanted in gastrocnemius muscle produced endometriosis-like lesions.
Lesions exhibited mechanical hyperalgesia and increased nociceptor firing *in vivo*.
Muscular invasion by endometrial cells and markers for nociceptors was observed.
Progesterone and leuprolide inhibited of mechanical hyperalgesia in cystic lesions.
This novel approach provides insight into our understanding of endometriosis pain.

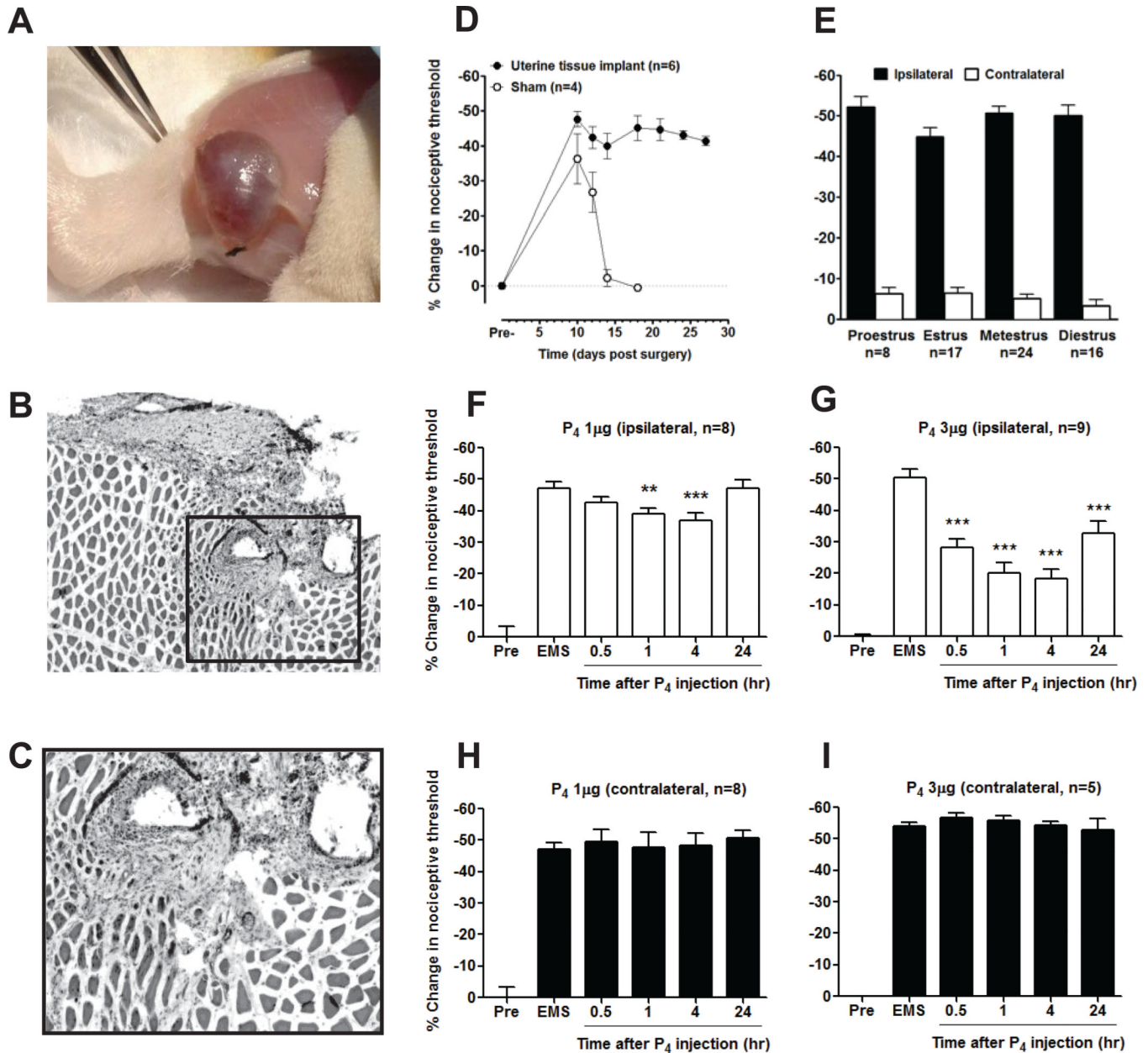


Figure 1. Morphologic and behavioral changes induced by ectopic uterine tissue. (A) 3 weeks after surgical implant of uterus tissue on the gastrocnemius muscle, surgical dissection reveals the gross anatomy of the cystic lesion and close muscular structures. (B) Microscopic analysis of cystic lesion reveals skeletal muscle invasion by ectopic endometrium and development of accessory cystic structures. Hematoxylin-eosin staining, 50X. (C) High magnification detail of panel B showing embedding of uterine tissue in skeletal muscle; Hematoxylin-eosin staining, 100X. (D) Mechanical hyperalgesia was already present at day 10 post-implantation after unilateral transplantation of endometrium, remaining undiminished for the duration of the testing period 27 days post-implantation. Hyperalgesia was significantly greater than in rats implanted with adipose tissue on to gastrocnemius muscle. (E) Mechanical hyperalgesia at the site of cystic lesion was evaluated at proestrus, estrus,

metestrus and diestrus. No significant difference in nociceptive threshold was observed after testing ipsilateral or contralateral to the implant. **(F)** Intralesional administration of progesterone (P_4) at doses of 1 μg , or **(G)** 3 μg at the site of the endometrial implant significantly attenuated mechanical hyperalgesia (repeated measures one-way ANOVA with Dunnett's multiple comparison test). **(H, I)** The same doses of progesterone had no effect on nociceptive mechanical threshold when injected in the contralateral side to the uterus implant. Behavioral data are presented as % of change of baseline values. $**P < 0.01$; $***P < 0.001$.

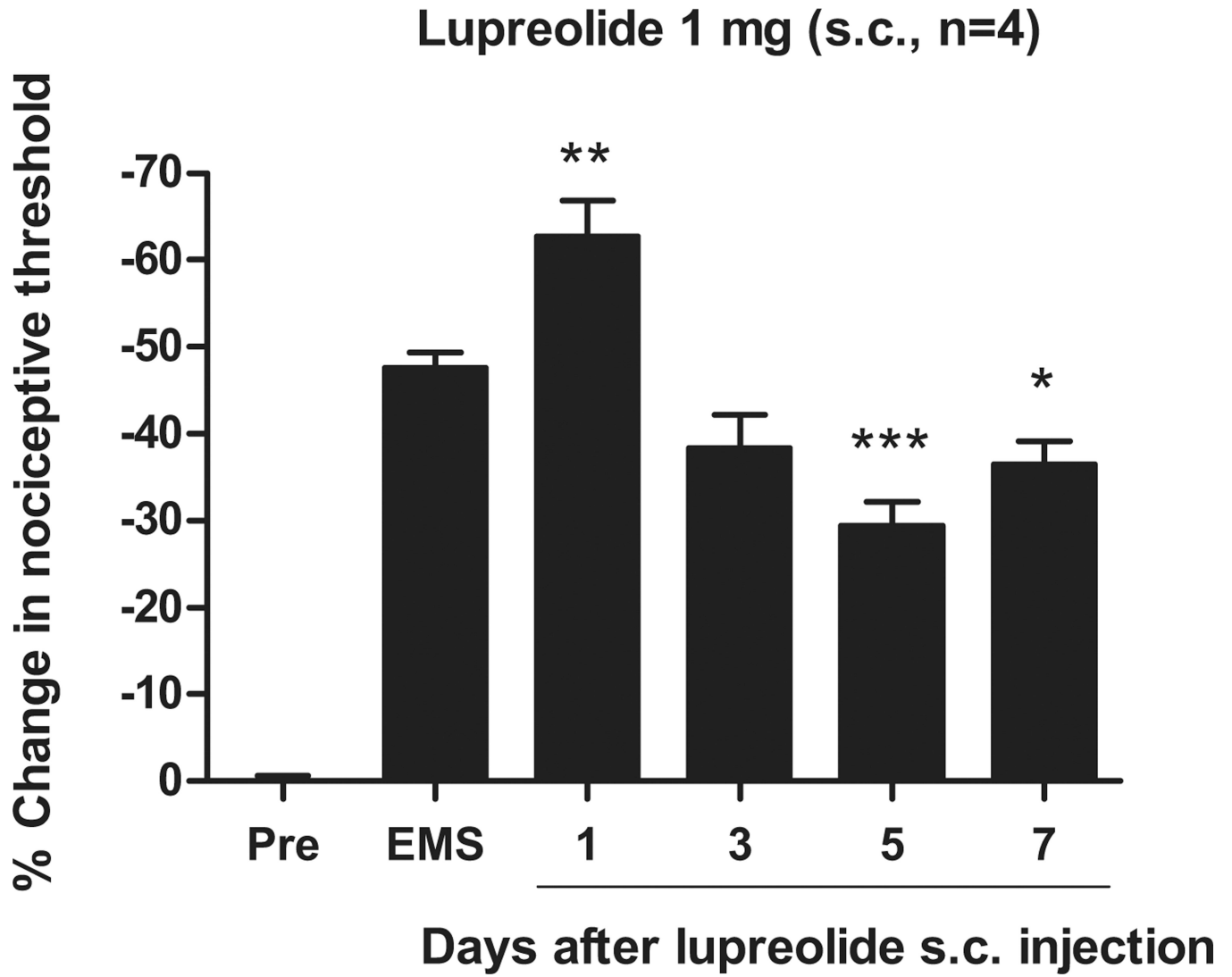


Figure 2.

Systemic administration of leuprolide modulates the mechanical hyperalgesia induced by ectopic endometrium. The s.c. administration of leuprolide produced a bi-phasic effect on mechanical hyperalgesia associated to endometriosis-like lesions: one day after injection such hyperalgesia was increased; then a progressive attenuation of the hyperalgesia was observed, which persisted at least until day 7 after leuprolide injection. * $P < 0.05$; ** $P < 0.01$; *** $P < 0.001$.

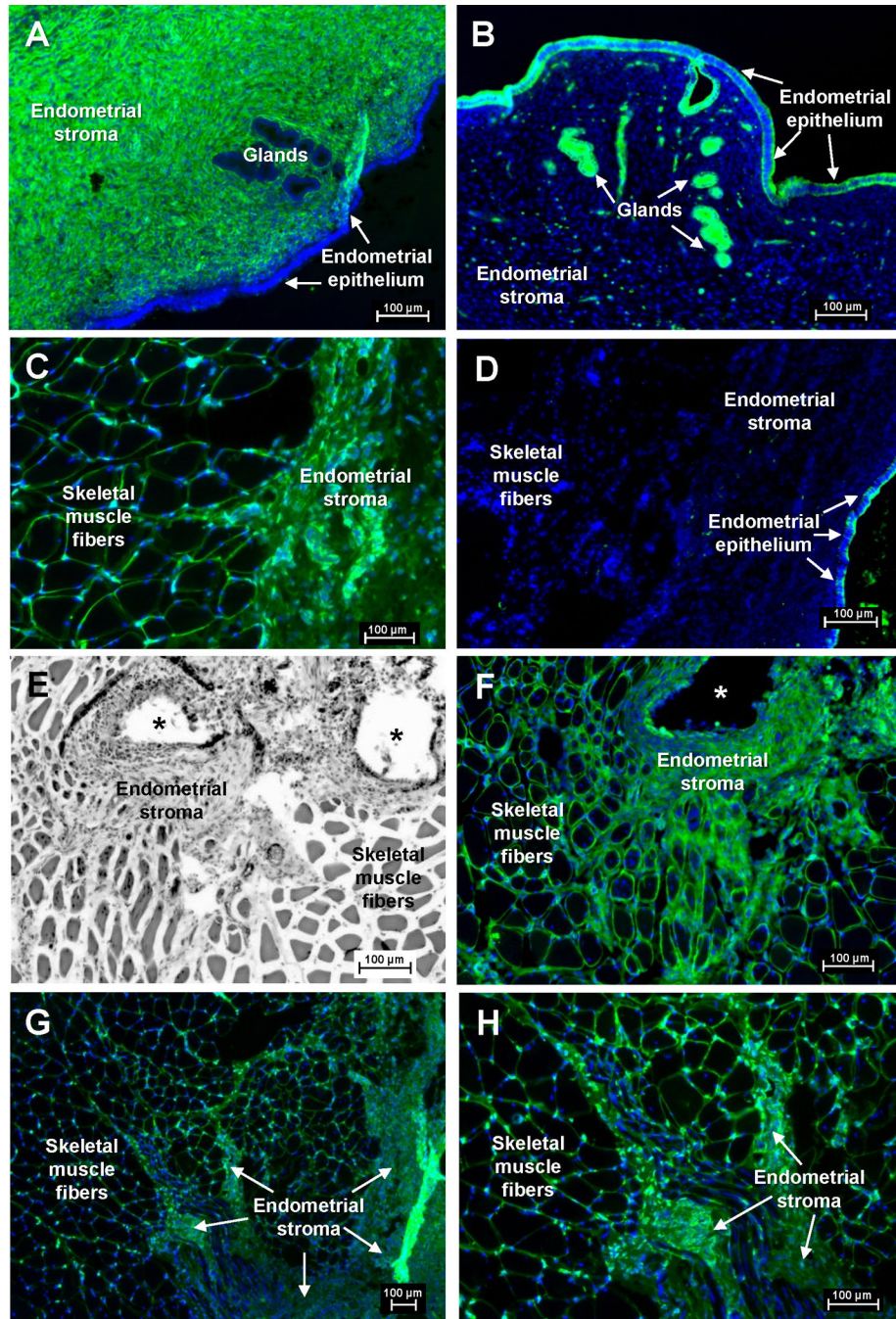


Figure 3. Comparative histologic study of eutopic endometrium and ectopic endometrial implants. (A) Rat eutopic uterus sample showing vimentin reactivity in endometrial stromal fibroblasts and unlabeled endometrial surface epithelium and glands (arrows). (B) Rat eutopic uterus sample showing cytokeratin 18 reactivity in endometrial surface epithelium and glands and lack of immunolabeling in endometrial stromal fibroblasts. (C) Uterine implant showing vimentin reactivity in endometrial stromal fibroblasts and endomysium, and non immunolabeled skeletal muscle fibers. (D) Cystic uterine implant showing cytokeratin 18 reactivity in the endometrial epithelium and non immunolabeled skeletal muscle fibers. (E)

Hematoxylin-eosin staining showing cystic structures (indicated by *) and endometrial stroma embedded into the skeletal muscle tissue. **(F)** Serial section from the same specimen in panel e showing vimentin positive elements infiltrating between the skeletal muscle fibers. **(G)** Low magnification of implant showing extensive invasion of muscle by vimentin-positive endometrial stromal fibroblasts. **(H)** High magnification detail of panel G showing vimentin-positive endometrial fibroblasts deeply invading endomysium and causing displacement and compression of the skeletal muscle fibers. Original magnifications 50X **(G)** or 100X **(A-F, H)**.

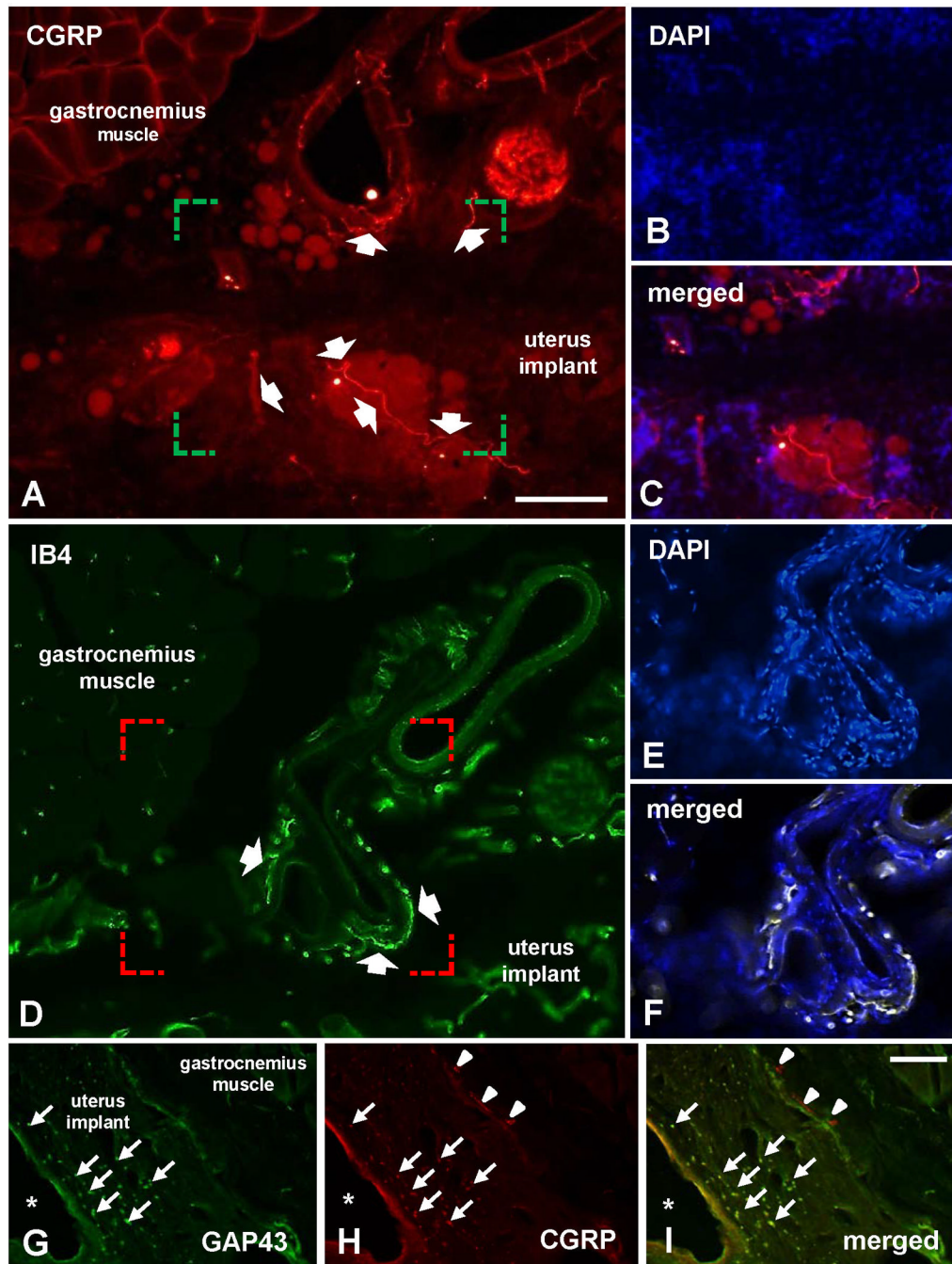


Figure 4.

Innervation of cystic lesions by muscle nociceptor and its axonal sprouts. Gastrocnemius muscle and ectopic uterine implant cyst immuno-labeled with antibodies against CGRP (A) and counterstained with DAPI (B, C); white arrows indicate nerve fiber-like structures. Gastrocnemius muscle and ectopic uterine implant cyst labeled with the IB4 (D) and counterstained with DAPI (E, F); white arrows indicate nerve fiber-like structures. (G) Immunolabeling for the marker for neuronal sprouting GAP43 is observed in the cyst wall. (H) Dot-like structures in the cyst wall and a nerve fiber-like structure surrounding the cyst are immune-positive to CGRP. (I) Merged image shows that only dot-like structures in the

cyst wall are co-labeled for GAP43 and CGRP. The cyst lumen is indicated by *. Scale bars represent 100 μm .

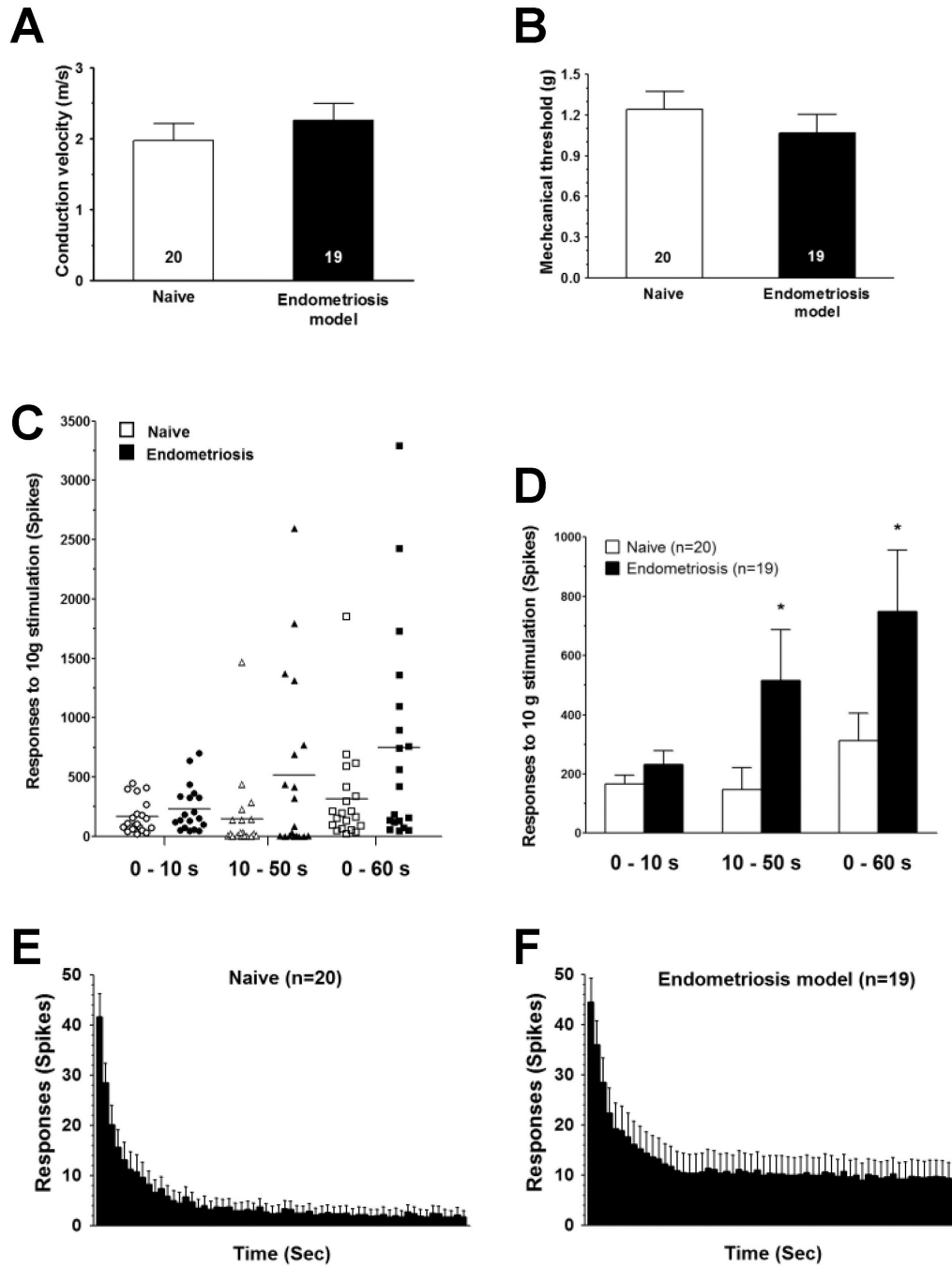


Figure 5. Sensitized nociceptors innervating ectopic uterine tissue. Two weeks after surgery, C-fiber uterine tissue implants, did not have a significant change in (A) mechanical threshold, or (B) conduction velocity. In contrast, they had significantly enhanced (C, D) C-fiber response to sustained mechanical stimulation (60 s), as revealed by increased number of spikes in recordings obtained during early (10 s) and late (50 s) parts of the stimulation period compared to control values obtained from naïve female rats. This was also evident in the time-course histograms of the C-fiber response, representing recordings obtained in naïve-control (E) and implanted (F) rats. Comparisons between naïve and implanted female rats

were made using one-tail Student's t-test for paired samples with Welch's correction; * $P < 0.05$.

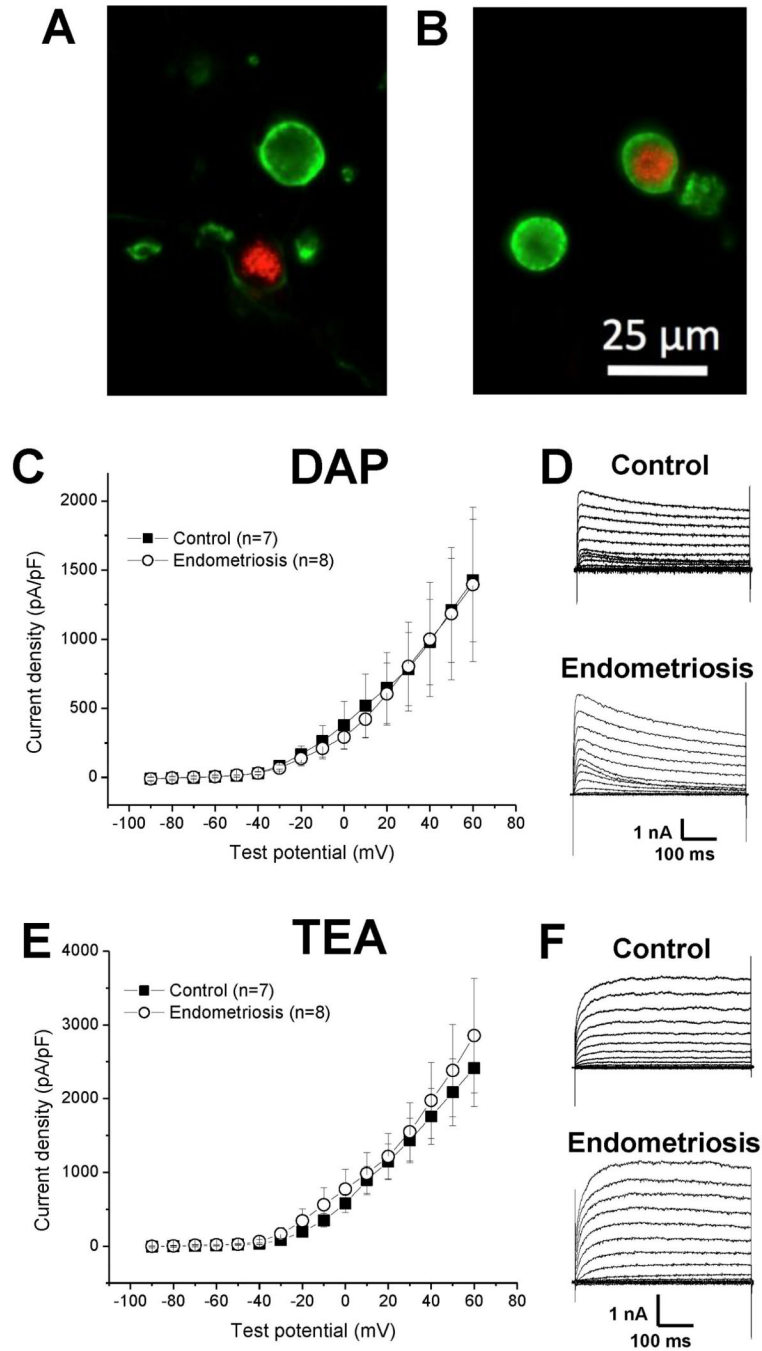


Figure 6.

A-type and DR-type potassium currents are not altered in cyst-innervating DRG neurons. Examples of retrogradely-labeled DRG cells with DiI (shown in red) and IB4-FITC labeling (shown in green) in culture: **(A)** a DiI labeled, IB4-negative DRG cell; **(B)** a double labeled (DiI labeled-IB4-positive) DRG cell. **(C)** Current-voltage curves (normalized to cell capacitance) representing A-type (sensitive to 3,4-diaminopyridine, DAP) current densities are shown. The peak current density in endometriosis DRG neurons (open circles, n=7) was not significantly different to that of control neurons (closed squares, n=7). **(D)** Representative current traces obtained from DRG neurons of control rats and rats submitted

to the endometriosis pain model in the presence of DAP. **(E)** The DR-type potassium current-density curves obtained in the presence of tetraethylammonium (TEA) were not significantly different in endometriosis DRG neurons (open circles, n=8) compared to control (closed squares, n=7). **(F)** Representative current traces obtained from DRG neurons of control rats and rats submitted to the endometriosis pain model in the presence of TEA.

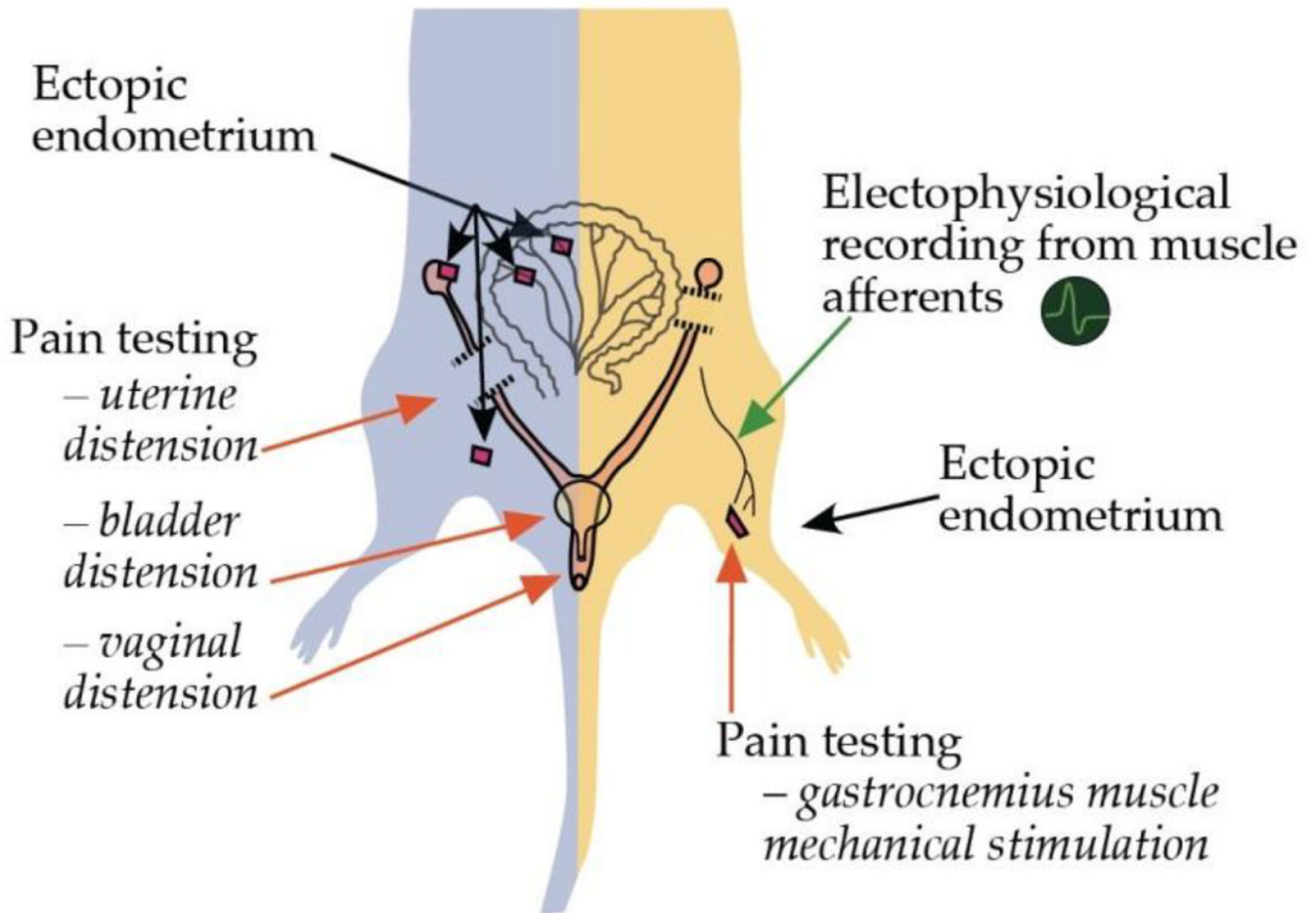


Figure 7.

Comparison of rat models of endometriosis pain. The rat model developed by Vernon and Wilson (1985) and adapted by Berkley and colleagues (2001) for the behavioral assessment of endometriosis pain (left side of the figure), differs in several ways from the model presented here (right side of the figure). In the former model of endometriosis pain, ectopic uterine tissue is implanted in the peritoneal cavity and nociceptive testing performed by mechanical stimulation of non-implanted structures (i.e., uterine, bladder or vaginal distension). In contrast, the model presented here allows direct nociceptive testing of uterine tissue-implanted gastrocnemius muscle, as well as, electrophysiological recording from nociceptive afferents innervating the ectopic uterine tissue and local testing of putative modulatory agents. Additional advantages include: (1) easy access for retrograde labeling of DRG neurons innervating from endometriosis-like lesions allowing for morphological and *in vitro* electrophysiological studies and, (2) contralateral assessment of nociceptive responses or drug administration in order to evaluate for extra-local effects of putative modulators.